

## SUPPLEMENTARY FIGURE LEGENDS

### **Figure S1. AcrIIA2 Directly Interacts with sgRNA-bound SpyCas9 and Inactivates SpyCas9.**

#### **Related to Figure 1.**

(A) *In vitro* enzymatic assay monitoring cleavage of linear dsDNA by SpyCas9 and sgRNA in the presence of AcrIIA2. The molar ratios of AcrIIA2:SpyCas9 are shown at the top of each lanes.

(B) AcrIIA2 selectively forms a stable complex with sgRNA-bound SpyCas9 rather than apo or DNA-bound SpyCas9-sgRNA in solution. SEC was performed using SpyCas9 in the presence or absence of sgRNA and sgRNA-dsDNA.

(C) AcrIIA2 physically interacts with sgRNA-bound SpyCas9. MBP pull-down assays were performed using MBP-tagged SpyCas9 in presence or absence of sgRNA.

(D) Oligomeric state of AcrIIA2 in solution detected by SEC-MALS. The horizontal red line represents the SEC-MALS calculated mass for AcrIIA2. The calculated and theoretical molecular masses are 14.4 kDa and 14.2 kDa, respectively, indicating that AcrIIA2 exists as a monomer in solution.

### **Figure S2. Schematic of sgRNA in SpyCas9-sgRNA-AcrIIA4 Ternary Complex.**

#### **Related to Figure 2.**

(A) Schematic representation of the sgRNA scaffold.

(B) Structure of the sgRNA in the SpyCas9-sgRNA-AcrIIA4 ternary complex.

### **Figure S3. AcrIIA4 Targets the Surface Formed by RuvC, Topo, and CTD Domains.**

#### **Related to Figures 2 and 3.**

(A) Ribbon diagram of AcrIIA4 interacting with the concave surface formed by the Topo, CTD and RuvC domains. The bound AcrIIA4 is highlighted by a black circle.

(B) Electrostatic surface of the Topo, CTD and RuvC domains shown in the same orientation as in Figure S3A. The binding region for AcrIIA4 is highlighted by a black circle.

(C) Two ribbon view of AcrIIA4. AcrIIA4 in left panel is shown in the same orientation as in Figure S3A.

(D) Electrostatic surface of AcrIIA4 in the same orientation as in Figure S3C right panel.

(E) Charge reversal mutation analysis of AcrIIA4 residues involved in the binding to sgRNA-bound SpyCas9 by MBP pull-down assay of MBP-tagged AcrIIA4.

(F) *In vitro* enzymatic assay of charge reversal mutations of AcrIIA4 residues that impaired binding of AcrIIA4 to sgRNA-bound SpyCas9.

**Figure S4. Selective Recognition of SpyCas9-sgRNA Binary Complex by AcrIIA4 and AcrIIA2.**

**Related to Figures 2 and 4.**

(A) AcrIIA2 competitively binds to preformed SpyCas9-sgRNA binary complex (upper panel) but not to preformed SpyCas9-sgRNA-dsDNA ternary complex (lower panel) in EMSA assays. The molar ratios of AcrIIA2:SpyCas9 are shown at the top of the gel.

(B) Superposition of AcrIIA4 with dsDNA based on their respective ternary complexes. The position of +1 phosphate group and cleavage site in non-target DNA strand are pointed by black and red arrows, respectively. TS and NTS represent target and non-target DNA strands, respectively.

(C) Structural comparison of domain movement on proceeding from the apo-SpyCas9 to the SpyCas9-sgRNA binary complex. Vector lengths correlate with the domain motion scales.

(D, E, F) Overall structures (upper panels) and electrostatic surfaces (lower panels) of AcrF1 (panel D), AcrF2 (panel E) and AcrF3 dimer (panel F). The interaction regions for Csy (AcrF1 and AcrF2) or Cas3 (AcrF3) are highlighted by black circles.

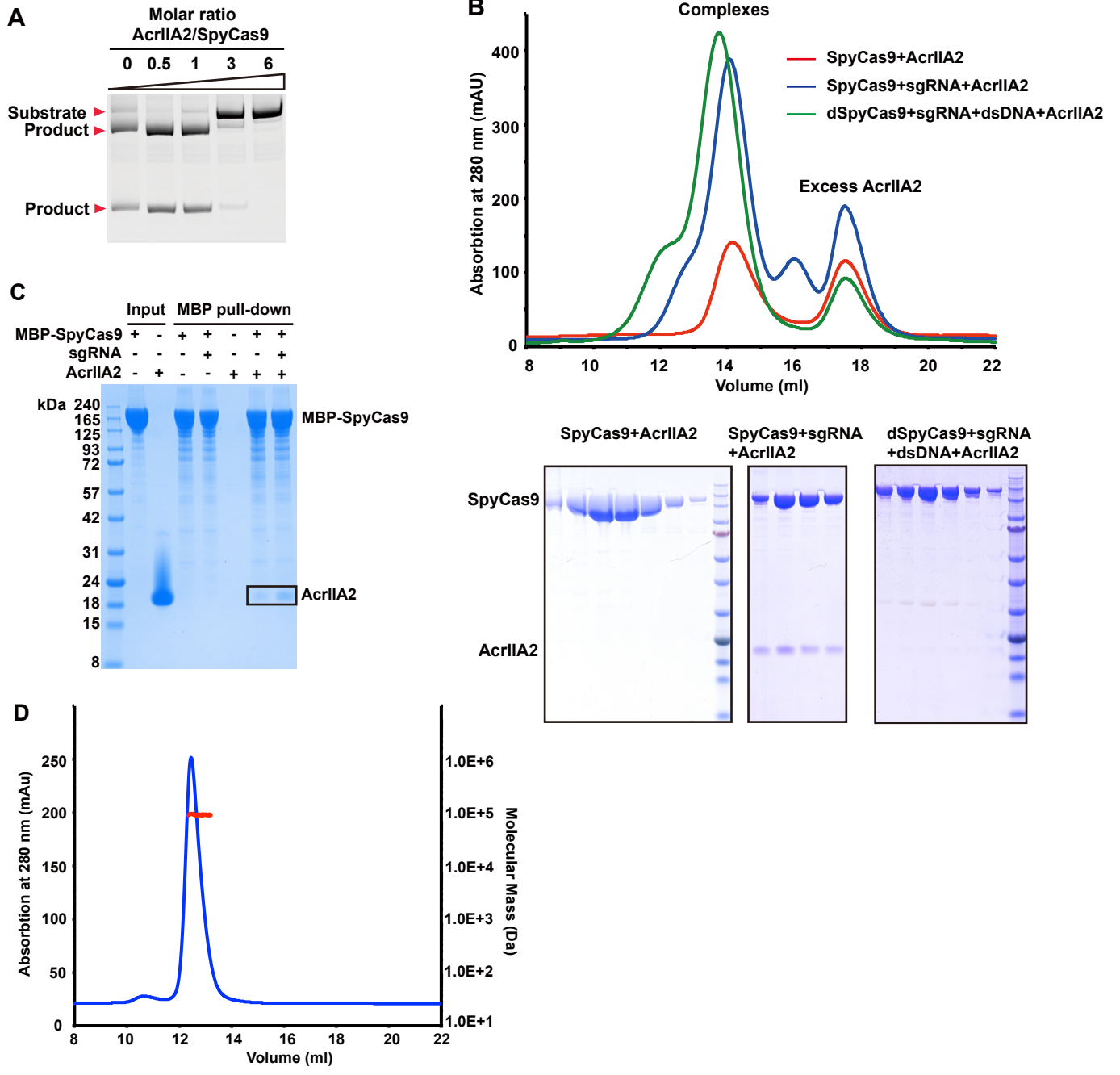


Figure S1

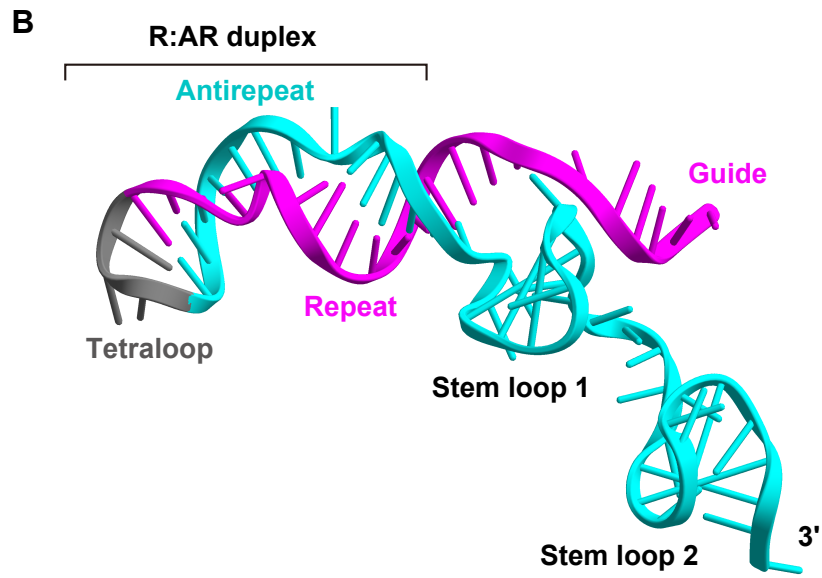
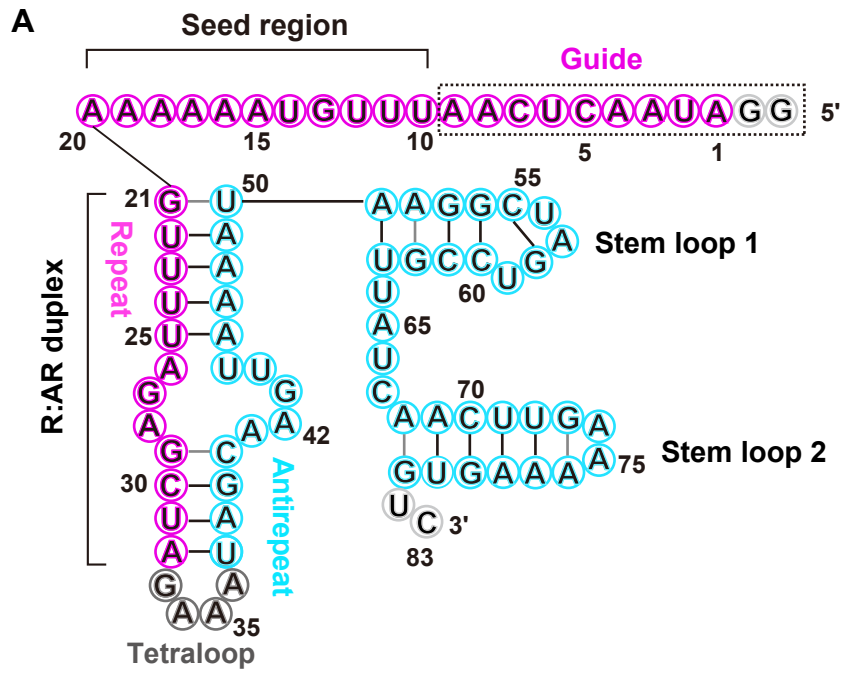
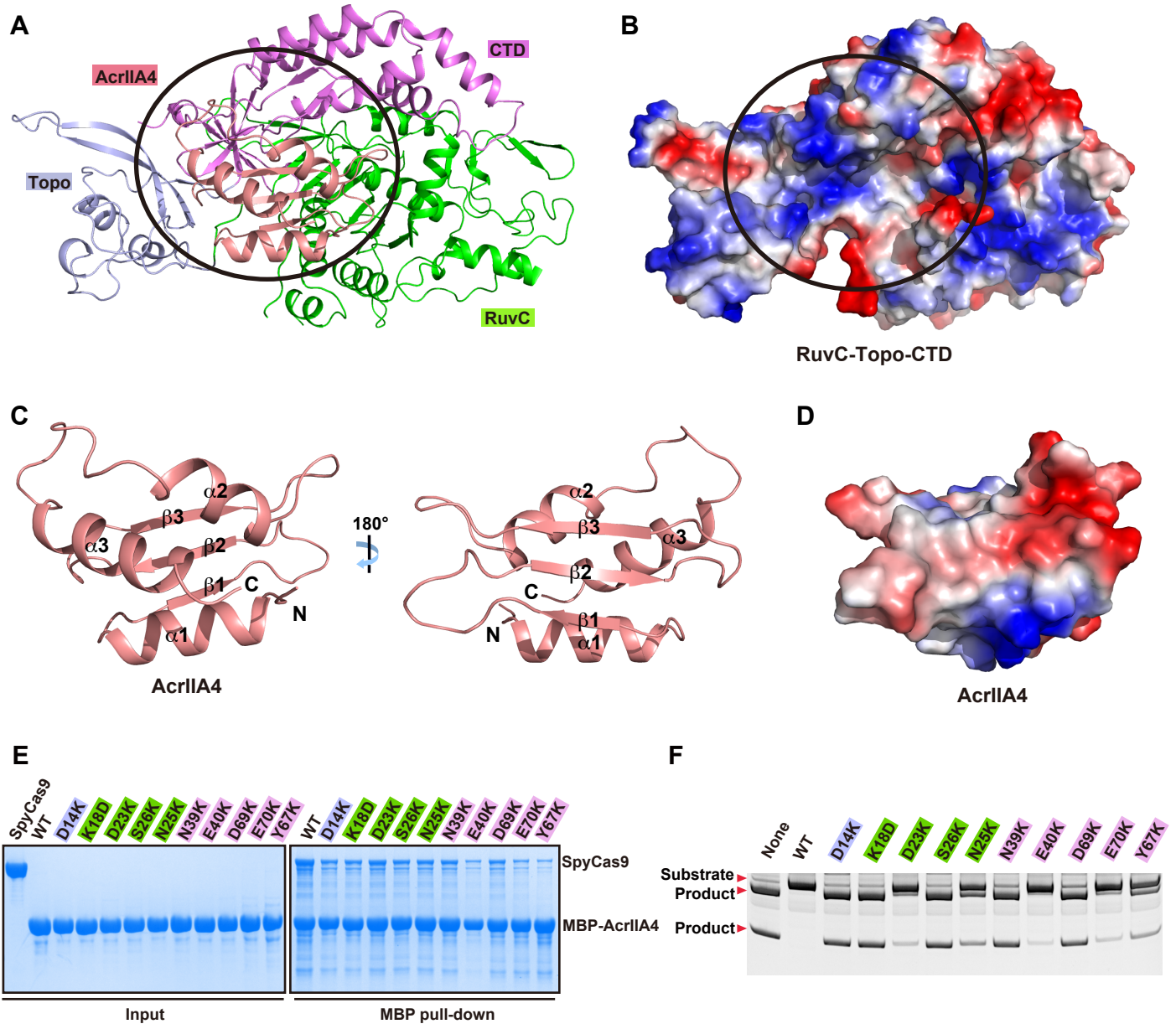


Figure S2



**Figure S3**

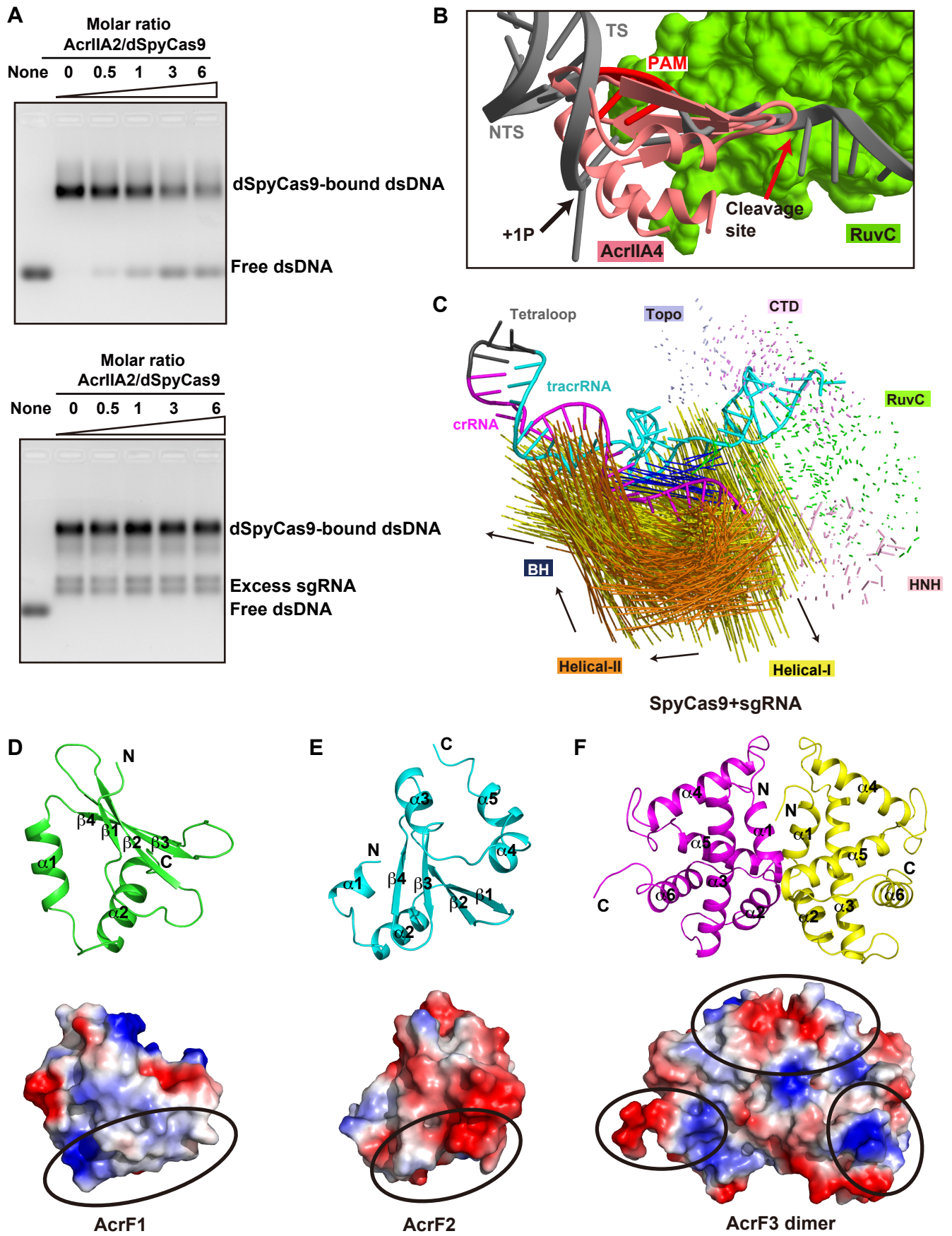


Figure S4